8-1-2023

Comprehensive molecular and clinical characterization of NUP98 fusions in pediatric acute myeloid leukemia

Eline J M Bertrums

Jenny L. Smith

Lauren Harmon

Rhonda E. Ries

Yi-Cheng J. Wang

See next page for additional authors

Recommended Citation

Bertrums EJM, Smith JL, Harmon L, et al. Comprehensive molecular and clinical characterization of NUP98 fusions in pediatric acute myeloid leukemia. Haematologica. 2023;108(8):2044-2058. Published 2023 Aug 1. doi:10.3324/haematol.2022.281653

Comprehensive molecular and clinical characterization of *NUP98* fusions in pediatric acute myeloid leukemia

Eline J. M. Bertrums,[1,2,3*] Jenny L. Smith,[4*] Lauren Harmon,[5*] Rhonda E. Ries,[4] Yi-Cheng J. Wang,[6,7] Todd A. Alonzo,[6,7] Andrew J. Menssen,[8] Karen M. Chisholm,[9] Amanda R. Leonti,[4] Katherine Tarlock,[4,10] Fabiana Ostronoff,[11] Era L. Pogosova-Agadjanyan,[4] Gertjan J. L. Kaspers,[1,12,13] Henrik Hasle,[14] Michael Dworzak,[15,16] Christiane Walter,[17] Nora Mühlegger,[15] Cristina Morerio,[18] Laura Pardo,[8] Betsy Hirsch,[19] Susana Raimondi,[19] Todd M. Cooper,[10] Richard Aplenc,[20] Alan S. Gamis,[21] Edward A. Kolb,[22] Jason E. Farrar,[23] Derek Stirewalt,[4] Xiaotu Ma,[24] Tim I. Shaw,[24] Scott N. Furlan,[4] Lisa Eidenschink Brodersen,[8] Michael R. Loken,[8] Marry M. van den Heuvel-Eibrink,[1,25] C. Michel Zwaan,[1,2,13] Timothy J. Triche Jr.,[5,6,26] Bianca F. Goemans[1#]and Soheil Meshinchi[4,7,10#]

[1]Princess Máxima Center for Pediatric Oncology, Utrecht, the Netherlands; [2]Department of Pediatric Oncology/Hematology, Erasmus Medical Center – Sophia Children's Hospital, Rotterdam, the Netherlands; [3]Oncode Institute, Utrecht, the Netherlands; [4]Fred Hutchinson Cancer Research Center, Clinical Research Division, Seattle, WA, USA; [5]Department of Epigenetics, Van Andel Institute, Grand Rapids, MI, USA; [6]Department of Translational Genomics, University of Southern California, Los Angeles, CA, USA; [7]Children's Oncology Group, Monrovia, CA, USA; [8] Hematologics Inc., Seattle, WA, USA; [9]Department of Laboratories, Seattle Children's Hospital, Seattle, WA, USA; [10]Division of Hematology and Oncology, Seattle Children's Hospital, Seattle, WA, USA; [11]Intermountain Blood and Marrow Transplant and Acute Leukemia Program, Intermountain Healthcare, Salt Lake City, UT, USA; [12]Emma Children's Hospital, Amsterdam UMC, Vrije Universiteit Amsterdam, Pediatric Oncology, Amsterdam the Netherlands; [13]Dutch Childhood Oncology Group, Den Haag, the Netherlands; [14]Department of Pediatrics, Aarhus University Hospital, Aarhus, Denmark; [15]Children's Cancer Research Institute, Medical University of Vienna, Vienna, Austria; [16]St. Anna Kinderspital, Department of Pediatrics, Medical University of Vienna, Vienna, Austria; [17]Department of Pediatric Hematology and Oncology, University Hospital Essen, Essen, Germany; [18]Laboratory of Human Genetics, IRCCS Istituto Giannina Gaslini, Genoa, Italy; [19]Department of Pathology, St. Jude Children's Research Hospital, Memphis, TN, USA; [20]Division of Oncology and Center for Childhood Cancer Research, Children's Hospital of Philadelphia, Philadelphia, PA, USA; [21]Division of Hematology/Oncology, Children's Mercy Kansas City, Kansas City, MO, USA; [22]Nemours Alfred I. duPont Hospital for Children, Wilmington, DE, USA; [23]Arkansas Children's Research Institute and Department of Pediatrics, Hematology/Oncology Section, Department of Pediatrics, University of Arkansas for Medical Sciences, Little Rock, AR, USA; [24]Computational Biology Department, St. Jude Children's Research Hospital, Memphis, TN, USA; [25]Utrecht University, Utrecht, the Netherlands and [26]Department of Pediatrics, Michigan State University College of Human Medicine, Grand Rapids, MI, USA

**EJMB, JLS and LH contributed equally as first authors.*
#BFG and SM contributed equally as last authors.

Correspondence: Eline J. M. Bertrums
e.j.m.bertrums@prinsesmaximacentrum.nl

S. Meshinchi
smeshinc@fredhutch.org

Received: June 27, 2022.
Accepted: February 14, 2023.
Early view: February 23, 2023.

https://doi.org/10.3324/haematol.2022.281653

Abstract

NUP98 fusions comprise a family of rare recurrent alterations in AML, associated with adverse outcomes. In order to define the underlying biology and clinical implications of this family of fusions, we performed comprehensive transcriptome, epigenome, and immunophenotypic profiling of 2,235 children and young adults with AML and identified 160 *NUP98* rearrangements (7.2%), including 108 *NUP98-NSD1* (4.8%), 32 *NUP98-KDM5A* (1.4%) and 20 *NUP98*-X cases (0.9%) with 13 different fusion partners. Fusion partners defined disease characteristics and biology; patients with *NUP98-NSD1* or *NUP98-KDM5A* had distinct immunophenotypic, transcriptomic, and epigenomic profiles. Unlike the two most prevalent *NUP98* fusions, *NUP98*-X variants are typically not cryptic. Furthermore, *NUP98*-X cases are associated with WT1 mutations, and have epigenomic profiles that resemble either *NUP98-NSD1* or *NUP98-KDM5A*. Cooperating *FLT3*-ITD and *WT1* mutations define *NUP98-NSD1*, and chromosome 13 aberrations are highly enriched in *NUP98-KDM5A*. Importantly, we demonstrate that *NUP98* fusions portend dismal overall survival, with the noteworthy exception of patients bearing abnormal chromosome 13 (*clinicaltrials gov. Identifiers: NCT00002798, NCT00070174, NCT00372593, NCT01371981*).

Introduction

Acute myeloid leukemia (AML) accounts for 15-20% of all pediatric leukemias and is a very heterogeneous disease.[1,2] Besides early response to induction treatment assessed by morphology and flow cytometry-based measurable residual disease (MRD), cytogenetic and molecular aberrations are the most important prognostic factors that guide risk group stratification.[1,3] Although survival rates of pediatric AML (pAML) patients have improved significantly, over the last decade these have reached a plateau, with long-term survival rates around 70-80%.[3,4] A third of all pAML patients relapse, and their outcome is poor.[3] In addition, treatment-related toxicity and mortality make intensification of treatment challenging.[2,3] Thus, the identification of prognostic subgroups for risk group and treatment stratification is of utmost value to improve treatment and outcomes of specifically high-risk subtypes.[2] Due to the very low prevalence of some subgroups, studies to identify these cases can be challenging and therefore require international collaboration.

NUP98 (chromosome 11p15) encodes a nucleoporin protein, which is part of the nuclear pore complex.[5] *NUP98* was first shown to be fused to *HOXA9* in t(7;11) FAB (French-American-British classification) M2 and M4 AML in 1996.[6] In the last 20 years, over 30 different partner genes in AML and therapy-related myelodysplastic syndrome have been described.[7-10] NUP98 fusion proteins involve the N-terminal portion of NUP98 and the C-terminal portion of the fusion partner.[5] These fusion partners consist of homeodomain proteins, which are transcription factors, and non-homeodomain proteins, which are thought to play a role in transcriptional or epigenetic regulation.[5] In pAML patients, *NUP98* translocations with *KDM5A* and *NSD1* have been most frequently described.[11,12] These patients are now notorious for inferior outcome compared to non-*NUP98*-translocated patients and are treated as high-risk patients in most current treatment protocols.[9,13] However, *NUP98* translocations with other partners, here called *NUP98*-X, are rare, and their prognostic relevance is unknown; consequently, there is a necessity to define the optimal risk stratification and treatment strategy for these patients. Here, we present the molecular and clinical characteristics of *NUP98*-translocated pAML patients within four consecutive Children's Oncology Group (COG) trials and an International Berlin-Frankfurt-Münster AML study group (I-BFM AML SG) collaboration. We aim to define the clinical relevance for all *NUP98* translocations with cooperating mutations and copy number variants.

Methods

Patient samples

Patients enrolled in the COG trials CCG-2961, AAML03P1, AAML0531 and AAML1031 were eligible for this study. Details of these studies have been previously described.[14-17] In total, 3,493 patients were included in these studies, of which 2,235 were eligible for inclusion due to availability of comprehensive *NUP98* fusion, molecular, and clinical data (*Online Supplementary Figure 1; Online Supplementary Tables S1* and *S2*). For the remaining patients, these data were unavailable. In addition, we sent out an I-BFM AML SG proposal to include pediatric AML patients with a *NUP98*-X translocation from other study groups. Consent, in accordance with the Declaration of Helsinki, was obtained from all study participants. The Fred Hutchinson Cancer Research Center Institutional Review Board and the COG Myeloid Biology Committee approved and oversaw the conduct of this study. Adult AML patients from the Beat AML study, The Cancer Genome Atlas AML (TCGA LAML), and Southwestern Oncology Group (SWOG) AML studies were included as comparators for *NUP98* fusion analysis and details were reported accordingly in references.[18-23]

Screening of *NUP98* fusions

The *NUP98* fusions were detected by either karyotype or combined fusion detection algorithms STAR-fusion v1.8.1, TransAbyss v1.4.10, and CICERO v0.1.8[24-26] completed on RNA sequencing (RNA-seq). For differences in detection methods per COG trial, see the *Online Supplementary Appendix*. The majority (94%) of *NUP98*-translocated patients had RNA-seq evidence of their fusion. STAR-fusion was run using default parameters with the premade GRCh37 resource library with Gencode v19 annotations (*https://data.broadinstitute.org/Trinity/CTAT_RESOURCE_LIB/*). The TransAbyss software was executed with the GRCh37-lite reference genome with the following parameters included: fusion breakpoint reads ≥1, flanking pairs and spanning reads ≥2 counts. CICERO fusion detection was performed with default parameters with GRCh37-lite. Fusions detected computationally were verified using Fusion Inspector v.1.8.1 (Broad Institute, Cambridge, MA) and visualized on IGV[27-30] and BAMBINO.[31] Beat AML (n=440) and SWOG AML (n=206) transcriptome sequence reads were analyzed using STAR-fusion v1.8.1 with the same reference resource library and parameters as above.[24] TCGA LAML (n=179) RNA-seq fusion data were downloaded from supplementary materials.[19]

Statistical methods

Data were current as of March 31, 2019. The Kaplan-Meier method was used to estimate overall survival (OS, defined as time from study entry to death) and event-free survival (EFS, time from study entry until failure to achieve complete remission [CR] during induction, relapse, or death). Relapse risk (RR) was calculated by cumulative incidence methods defined as time from the end of induction I for patients in CR to relapse or death, where deaths without a relapse were

considered competing events. Patients who withdrew from therapy due to relapse, persistent central nervous system (CNS) disease, or refractory disease with >20% bone marrow blasts by the end of induction I were defined as induction I failures. MRD was defined at the end of course one using flow cytometry with a cut-off of 0.1% detection of disease. The I-BFM patients were excluded from survival analyses due to variation in study groups and treatment protocols.

Results

Clinical characteristics

Between 1995 and 2017, 3,493 AML patients were treated on consecutive COG trials CCG-2961, AAML03P1, AAML0531, and AAML1031, of which 2,235 were eligible for comprehensive outcome (see Methods) and cytomolecular association analyses. Within this cohort, 160 patients (7.2%) with a *NUP98* translocation were identified (Figure 1A); the remaining 2,075 patients were included as a reference cohort. In addition, six *NUP98*-X cases were included via the I-BFM AML SG, demonstrating that while rare, *NUP98*-X cases are present in multiple cohorts of patients. However, to prevent bias due to confounding variables, such as differences in study groups, fusion identification methods and treatment protocols, these patients were excluded from further analyses. Characteristics of all *NUP98*-X patients are depicted in the *Online Supplementary Table S3*.

The most common *NUP98* translocations were *NUP98-NSD1* (n=108) and *NUP98-KDM5A* (n=32; *Online Supplementary Figure S2A*). Furthermore, we identified 20 patients with 13 different *NUP98* translocation partners, including *HOXA9* (n=4), *HOXD13* (n=3), *PHF15* (n=2), *PHF23* (n=2) and single cases of *BPTF, BRWD3, DDX10, HMGB3, HOXA13, KAT7, PRRX1, SET,* and *TOP1* (Figure 1B). Interestingly, contrasting the cryptic *NUP98-NSD1* and *NUP98-KDM5A* fusions, an overwhelming majority of NUP98-X fusions were detectable as karyotypic variants with 17 of 20 (85%) having gross alterations by g-banding cytogenetics involving chr11p15.

Initial comparison of the *NUP98* fusion cohort to the reference patients demonstrated a significant sex bias in *NUP98* cases, with 61.3% being male *versus* 38.8% female (P=0.012) (Figure 1C). In particular, the *NUP98-NSD1* cohort contained 64.8% male *versus* 35.2% female patients. Additionally, *NUP98* fusions were enriched in children aged 3-10 years old (35.6%; P=0.005). Clinical characteristics for *NUP98*-translocated subgroups are summarized in Figure 1C-E and the *Online Supplementary Table S1*. In *NUP98-NSD1*-translocated patients, white blood cells and blast cell counts were both significantly higher, while in *NUP98-KDM5A* patients a reverse trend was seen. Classification by conventional cytomolecular stratification schemas, as previously described,[17] revealed that 39% of *NUP98-NSD1* patients had been classified as standard-risk (SR) and 61% as high-risk (HR). In contrast, most *NUP98-KDM5A* patients (97%) and *NUP98*-X patients (95%) were classified as SR.

Comparison of *NUP98* translocations with age at diagnosis based on fusion partners (Figure 1C) showed that *NUP98-NSD1* cases had a median age of 10.2 years (reference cohort 10.0; P=0.228), whereas *NUP98-KDM5A* cases had a median age of 2.7 years (P<0.001). *NUP98*-X patients showed a median age of 7.9 years (P=0.30) with a bi-modal distribution; 40% of the patients were under 3 years and 50% over 5 years with no patients over 18 years old (*Online Supplementary Figure S2B, C*). Almost all *NUP98*-X patients with homeobox fusion partners (n=9) were over 3 years old (8/9), with one exception (*NUP98-HOXD13*; P=0.025).

From Beat AML, TCGA LAML and SWOG, 825 adult AML cases were screened for *NUP98* fusions by RNA-seq fusion detection algorithms. Zero *NUP98-KDM5A*, 11 (1.3%) *NUP98-NSD1*, and two (0.2%) NUP98-X fusions were identified (*NUP98-TOP1* and *NUP98-RAP1GDS1*). These results demonstrate that *NUP98* rearrangements are less common, but still present, in older adult AML patients (13/825, 1.6%) compared to pediatric and young adult AML patients (160/2,235, 7.2%; P<0.001; *Online Supplementary Figure S2D*)[9].

Implications of variation of fusion junction

Analysis of *NUP98* fusion breakpoints by RNA-seq revealed a high diversity of *NUP98* exon junctions. Nearly 85% of *NUP98* fusions had a breakpoint junction in exon 12 (39.7%) or 13 (44.9%), while the remaining breakpoints occurred in various positions from exon 11 to exon 29 (*Online Supplementary Figure S2E*). Exon junctions correlated with the fusion partner, and *NUP98-NSD1* fusions primarily had exon 12 (52.9%) and 13 (43.23%) junctions (Figure 1F). However, exon 14 breakpoints were almost uniformly restricted to *NUP98-KDM5A* compared to other NUP98 fusions (P<0.001). *NUP98*-X cases showed a larger variability in *NUP98* exon breakpoints (*Online Supplementary Table S4; Online Supplementary Figure S3*). *NUP98* homeobox gene fusions were enriched in exon 12 breakpoints (6/9, 66%), while *PHF15* (n=2), *PHF23* (n=2), and *TOP1* partners had exon 13 breakpoints. Besides the commonly included nucleoporin FG repeat domains of the NUP98 protein, a minority of cases (n=3) included a larger portion of the protein with nucleoporin autopeptidase or, additionally, the Nup96 domains (Figure 2A).

Immunophenotypes

NUP98 fusions were previously reported to be associated with erythroid and megakaryocytic phenotypes.[10,32] Upon morphology, we identified that only *NUP98-KDM5A* fusions were more often associated with the FAB M6/M7 category compared to the reference cohort (46.9% *vs*. 5.5%; P<0.001). Additionally, the immunophenotype of *NUP98* fusions was examined using multidimensional flow cytometry.[33] *NUP98-NSD1* patients expressed early progenitor

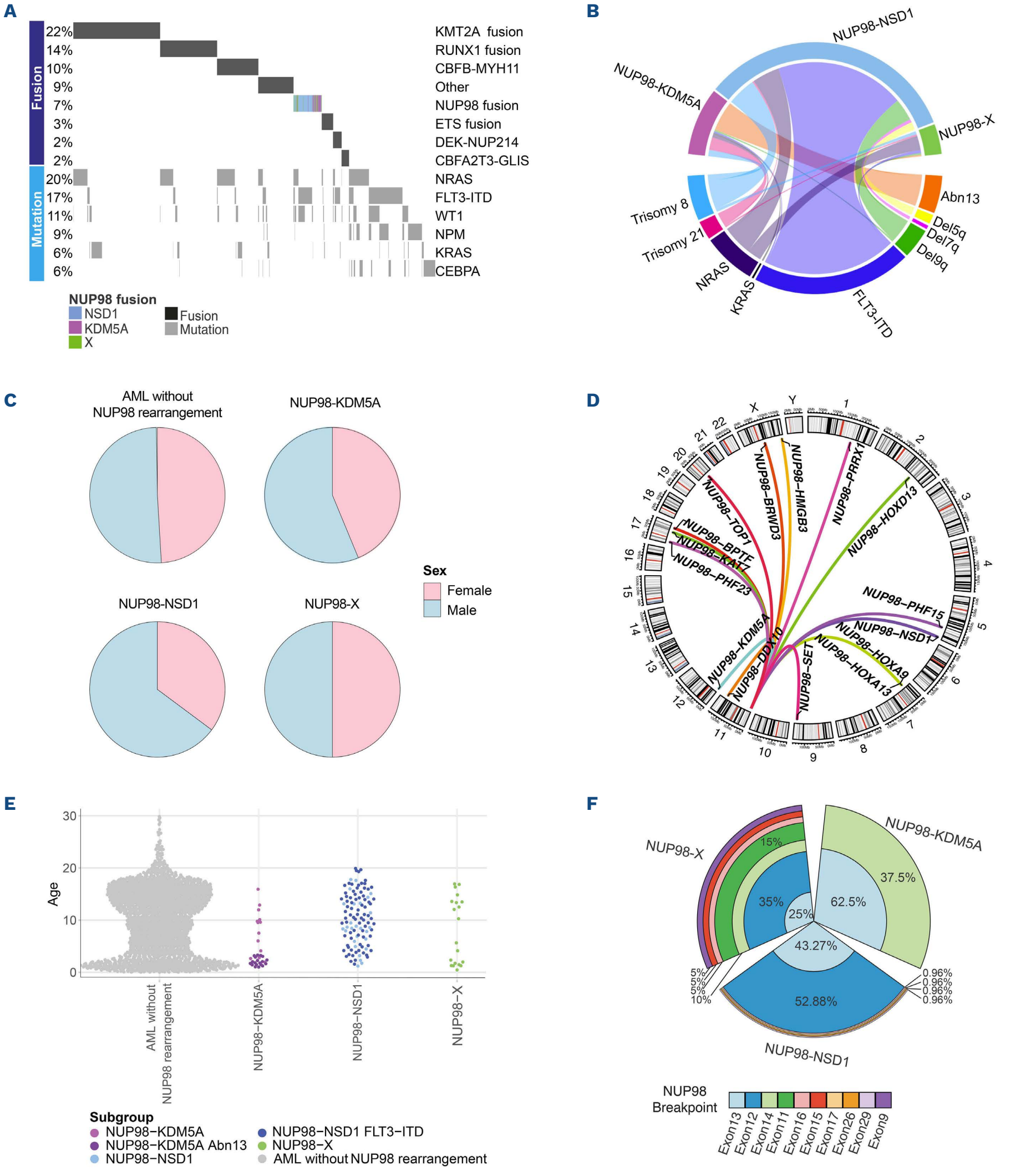

Figure 1. Clinical characteristics of patients with and without *NUP98* translocations. (A) Oncoprint depicting the major drivers of pediatric acute myeloid leukemia (AML) patients. (B) Circos plot depicting commonly co-occurring mutations and cytogenetic abnormalities in *NUP98*-translocated pediatric AML patients. (C) Pie charts depicting the sex divisions of patients in the *NUP98*-translocated AML subgroups. (D) Circos plot representing different fusion partner genes of *NUP98*-X translocations in pediatric AML patients. (E) Age distribution of AML patients. (F) Barchart (polar axis) illustrating the prevalence of *NUP98* exon junctions in *NUP98*-translocated AML. The Figure legend is ordered by decreasing *NUP98* exon prevalence in the *NUP98* fusion-positive cohort.

markers such as CD34 and CD117 (Figure 2B; *Online Supplementary Figure S4*). Patients harboring *NUP98-NSD1* and *FLT3* internal tandem duplication (-ITD) retained the immature markers but also showed evidence of monocytic maturation compared to *NUP98-NSD1* without *FLT3*-ITD, as demonstrated by expression of CD11b (84%), CD36 (55%) and CD64 (71%) (*Online Supplementary Table S6*). Nevertheless, *NUP98-NSD1* associated phenotypes were not as specific, or consistent, as seen in *NUP98-KDM5A*. The *NUP98-KDM5A* immunophenotype corresponded to megakaryocytic maturation, with at least partial expression of CD36, and absence of pluripotent markers CD34 and CD123. Notably, *NUP98-KDM5A* patients showed clusters that associated with co-occurrence of abnormal chromosome 13q (Figure 2C), demonstrating that these subsets of patients display a unique immunophenotype. Finally, *NUP98*-X fusions lacked consistent immunophenotype, aside from the majority expressing markers of early progenitors.

Cooperating karyotypic and molecular variants

Diagnostic specimens were evaluated for common translocations, chromosomal aberrations and common mutations, namely *FLT3*-ITD, *WT1, NPM1, CEBPA, KIT* and *CBL* mutations (Figures 1A and 2C). We confirmed the well-known enrichment of *FLT3*-ITD (74%) and *WT1* mutations (42%) in the *NUP98-NSD1* cohort.[5] Almost half of *NUP98-NSD1* patients with *FLT3*-ITD also harbored a *WT1* mutation, indicating triple positivity for adverse outcome variants in AML.[34] *NUP98-NSD1* patients also had a significant association with trisomy 8 (18.8%) compared to the reference cohort (5.3%; *P*<0.001). *NUP98-KDM5A* displayed a paucity of cooperating mutations. *NUP98*-X patients showed a higher prevalence of *WT1* mutations compared to the reference cohort (25% *vs*. 9.6%; *P*=0.039), associated with a higher age at diagnosis (median age 16.3 *vs*. 2.3 years; *P*=0.032).

We identified a notably high correlation of *NUP98-KDM5A* with chromosome 13 (chr13) structural variants, including del(13q), monosomy 13 and chr13 translocations. Abnormal chr13 (*NUP98-KDM5A*/13abn) was identified in 19 *NUP98-KDM5A* patients (63.3% *vs*. 2.3% in the reference cohort; *P*<0.001). *NUP98-KDM5A*/13abn were significantly younger than *NUP98-KDM5A*/13normal patients (median age 1.8 *vs*. 9.6 years; *P*<0.001). Thirteen *NUP98-KDM5A* patients (43.3%) patients harbored del(13q) *versus* one *NUP98*-X patient (*NUP98-SET*). Monosomy 13 (2/32) and translocation 13 (4/32) occurred less frequently in *NUP98-KDM5A* and were not found in *NUP98-NSD1* or *NUP98*-X (*Online Supplementary Table S5*).

The majority of del(13q) in *NUP98*-translocated cases (92%) began at band 13q12; the deletions ranged from 8 Mb to 59.5 Mb to the entire chromosome. The minimal commonly deleted segment was del(13)(q14.2q14.3), containing the *RB1* tumor suppressor gene (*Online Supplementary Figure S5*). *RB1* loss has been previously reported in patients with *NUP98-KDM5A*;[10] however, we demonstrated a much larger region of copy number alterations, including numerous additional genes. Of *NUP98-KDM5A*/13abn patients, 84% (16/19) had *NUP98* exon 13 breakpoints, suggesting that specific *NUP98* exon breakpoints in the fusion transcript may be linked to the presence of additional cytogenetic abnormalities. Finally, all ten acute megakaryoblastic leukemia (AMKL; FAB M7) *NUP98-KDM5A* cases with karyotype data available had chr13 alterations compared to three AMKL cases without *NUP98* fusions (*P*<0.001).

Gene expression profiling

Unsupervised hierarchal clustering of gene expression in *NUP98*-translocated patients and a reference cohort of known fusions including *KMT2A, CBFB-MYH11, RUNX1-RUNX1T1* and *DEK-NUP214*, as well as 84 healthy controls (n=988), revealed that the majority of *NUP98-NSD1* (n=104), *NUP98-KDM5A* (n=32), and the reference cohort cluster by fusion identity, while no uniform clustering of *NUP98*-X was observed (n=20) (Figure 3A). In order to further understand transcriptional similarities and differences between the diverse *NUP98* fusions, uniform manifold approximation and projection (UMAP) was completed on the *NUP98*-translocated patients' gene expression data (n=156). The Leiden algorithm[35] identified five transcriptional clusters. *NUP98-NSD1* patients clustered together, clearly separated from the majority of *NUP98-KDM5A* patients (Figure 3B). *NUP98*-X patients were dispersed, clustering more closely with *NUP98-NSD1* cases. The largest proportion of *NUP98*-X clustering together included seven homeobox and both *PHF23* partners, suggesting transcriptional similarities between *NUP98-HOX* fusions (cluster C3). The next cluster most associated with *NUP98*-X (cluster C5) included the majority of non-AMKL *NUP98-KDM5A* cases.

UMAP revealed segregation based on an AMKL and age-based signature (cluster C4), which embodied 78.6% of AMKL *NUP98*-translocated patients, all 3 years old or younger. The cluster primarily contained *NUP98-KDM5A* (22/32) cases and was enriched in *NUP98* exon 13 breakpoints. *NUP98*-X patients in C4 included single cases of *NUP98-SET* with del(13q), *NUP98-BPTF* with AMKL morphology, and NUP98-DDX10. Additionally, C4 included all *NUP98-KDM5A*/13abn cases (*Online Supplementary Figure S6A*), separating *NUP98-KDM5A* with and without chr13 abnormalities. Conversely, in a separate UMAP including heterogenous pAML fusions (N=1,482), this abn13-based clustering was not observed for non-*NUP98*-translocated subtypes (*Online Supplementary Figure S6B*).

Differential expression analysis compared *NUP98*-X directly to *NUP98-NSD1* and *NUP98-KDM5A* individually. Expression of *MECOM* and *PRDM16*, known prognostic markers in adult and pediatric AML,[36] effectively separated

Figure 2. Cytogenetics of *NUP98*-translocated pediatric acute myeloid leukemia. (A) Locations of breakpoints across the *NUP98* gene for all *NUP98*-translocated acute myeloid leukemia (AML). (B) Oncoprint depicting additional copy number variations (CNV) and mutations in *NUP98*-translocated patients. (C) Heatmap depicting the presence and absence of flow-cytometry immunophenotype markers in *NUP98*-translocated AML groups. *NUP98-HOX*-like fusions include fusion partners *HOXA9, HOXA13, HOXD13*, and *PRRX1*. *NUP98*-Reader-like fusions include fusion partners *BPTF, BRWD3, DDX10, HMGB3, KAT7, PHF15, SET,* and *TOP1*.

A

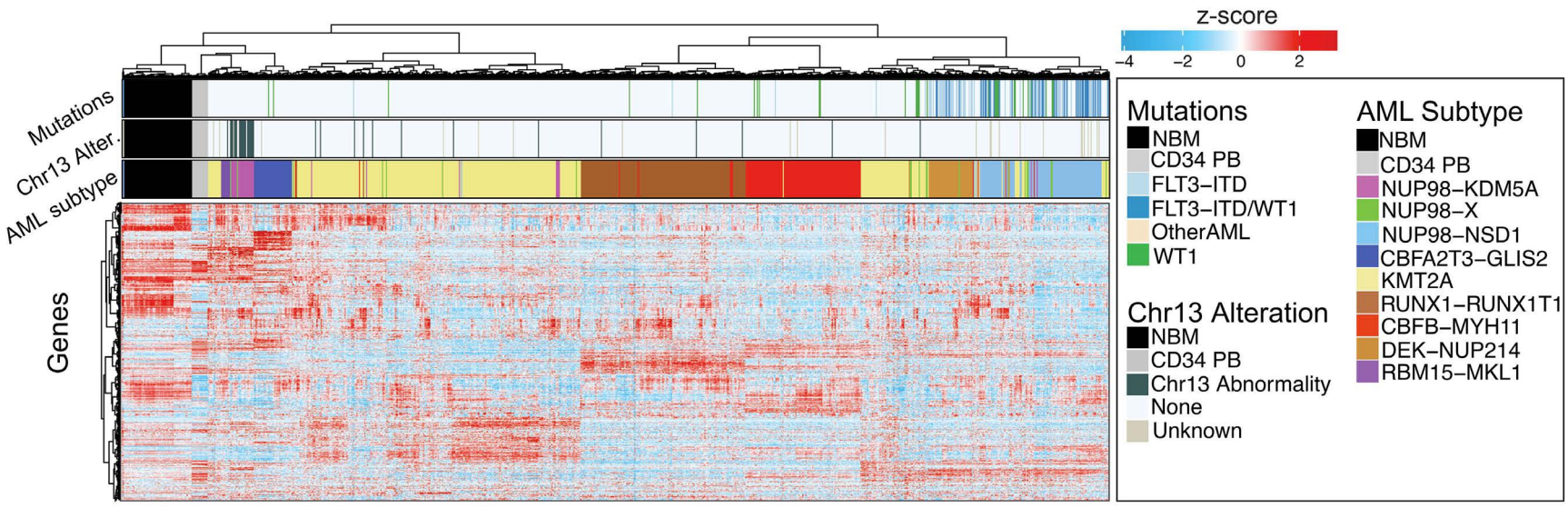

B

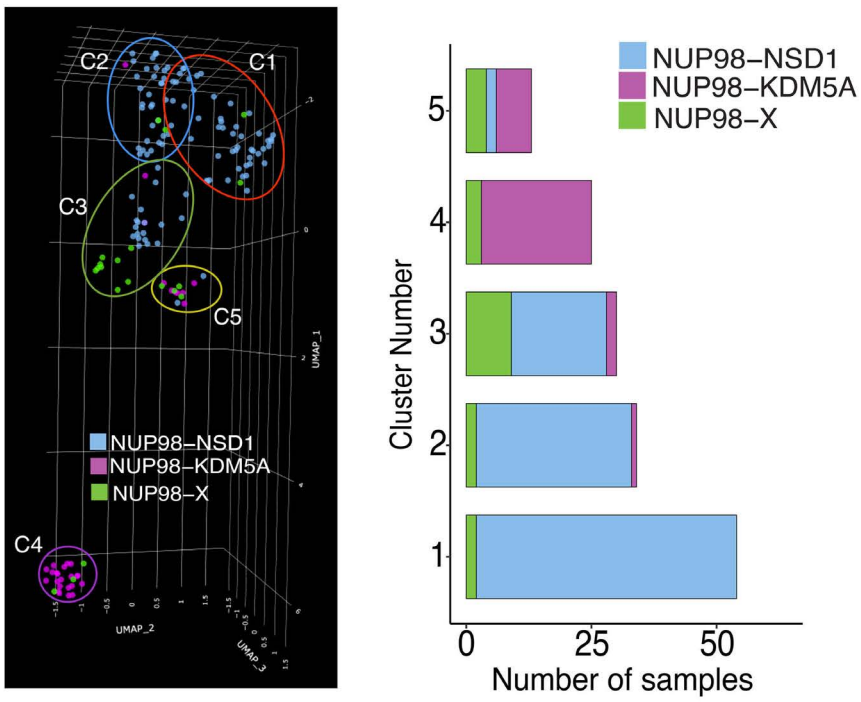

C

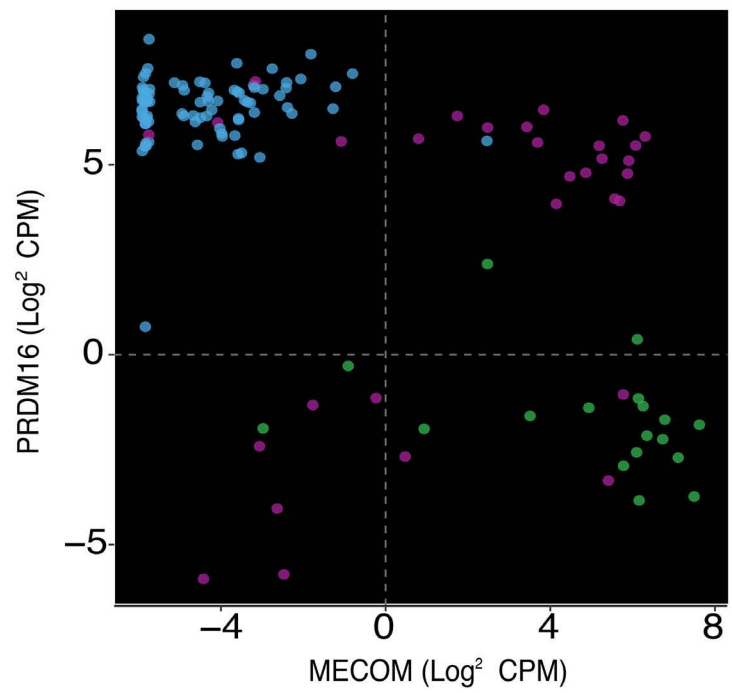

D

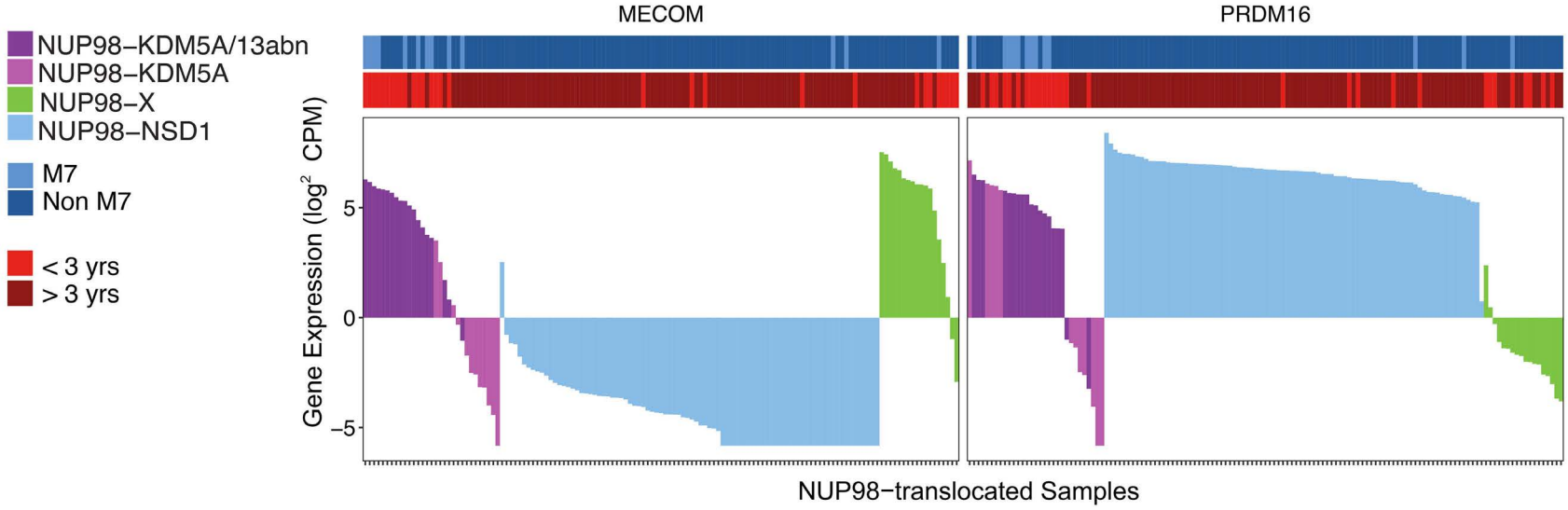

Figure 3. Expression pattern of pediatric acute myeloid leukemia with various *NUP98* translocations. (A) Unsupervised hierarchical clustering by gene expression including heterogenous pediatric acute myeloid leukemia (AML) subtypes, *NUP98*-translocated subgroups, normal healthy bone marrows (NBM) and CD34^{+} peripheral blood cells (CD34 PB). Annotation bars show AML subtype and co-occurring mutations. (B) Uniform manifold approximation and projection (UMAP) of gene expression, followed by Leiden clustering, for *NUP98*-translocated pediatric AML samples identifies five different transcriptional clusters. *NUP98* fusions are indicated in different colors: *NUP98-KDM5A* in purple, *NUP98-NSD1* in blue, and *NUP98*-X in green. (C) Expression of *MECOM* and *PRDM16* genes in different subgroups of *NUP98*-translocated pediatric leukemia. Same identification colors for *NUP98* fusions as in (B) are used. (D) Expression of stemness marker genes in all *NUP98*-translocated samples. Top bars represent French-American-British (FAB) classification and age category.

the *NUP98* subgroups (Figure 3C). Interestingly, about two-thirds of *NUP98-KDM5A* highly expressed both genes, while *NUP98*-X and *NUP98-NSD1* almost exclusively overexpressed one or the other (Figure 3D). *NUP98-KDM5A* patients with low *MECOM* and low *PRDM16* expression almost uniformly lacked chr13 alterations. Additionally, *NUP98-KDM5A*/13abn patients had reduced expression of genes in the involved area, including RB1 (P<0.001), *DLEU7* and *SPRYD7* (*Online Supplementary Figure S6C*).

We attempted to identify transcriptional signatures that might be shared between all *NUP98*-translocated cases and performed differential expression analysis comparing each group (*NUP98*-X, *NUP98-NSD1*, and *NUP98-KDM5A*) independently to the reference cohort (n=1,326) (Figure 4A). This analysis confirmed high inter-patient variability of *NUP98*-X fusions (*Online Supplementary Figure S7*). Gene expression profiling revealed 27 differentially expressed genes (DEG) exclusively shared between *NUP98*-X and *NUP98-NSD1*, including upregulation of *DNMT3B*, *MYCN*, and *PBX3* (Figure 4B). Within *NUP98-KDM5A*, a bimodal expression pattern of *DNMT3B* and *MYCN* was related to chr13 alterations, where cases lacking chr13 aberrations had decreased expression. *NUP98-X* and *NUP98-KDM5A* exclusively shared 26 dysregulated genes, including overexpression of *MLLT3, IRX3*, and *CD79a*.

The *NUP98*-translocated cohort had 38 DEG in common, including upregulation of numerous *HOX* genes. Among these 38 genes, 15 were also dysregulated in *NUP98*-translocated cohorts compared to healthy bone marrow samples. This minimal set of 15 genes strongly implicated dysregulation at the *HOX* loci; these targets include *HOXA* (chr7p15), *HOXB* (chr17q21), *hsa-mir-10a* (chr17q21), and *CACNG4* (chr17q24) transcripts (Figure 4C). *NUP98*-X cases expressed *HOXA/B* genes regardless of their fusion partner, and 60% (12/20) expressed both *HOXA/B* while the remaining third primarily overexpressed the *HOXA* cluster (*Online Supplementary Figure S8*). Overexpression of *HOX* genes and *hsa-mir-10a* was previously reported in *NUP98-KDM5A* and *NUP98-NSD1* and is now shown to be a common feature of *NUP98* translocations.[9,13]

Single-sample gene-set enrichment analysis (ssGSEA) addresses the inherent variability within diverse *NUP98* fusions and was performed to investigate alterations in the expression of down-stream targets of *hsa-mir-10a* and HOX transcription factors.[37] *NUP98*-translocated subgroups had significantly lower enrichment scores of *miR-10a-3p* and *miR-10a-5p/miR-10b-5p* target genes, an indication of negative regulation, compared to normal bone marrow samples (P<0.001). Investigation of HOX transcription factor (TF) pathways by ssGSEA, revealed enrichment in *HOXB8* molecular interactions (adj.P<0.008). The *HOXB8* pathway included well known HOX transcriptional co-factors *MEIS1, MEIS2, PBX1, PBX3, PBX3*,[38] and the proto-oncogene *RAF1*. *NUP98*-X and *NUP98-KDM5A* exhibited a positive enrichment of *HOXA9* interacting partners (P<0.001; Figure 4D). Additionally, we employed RCIS-Target to identify TF motifs enriched in the overexpressed genes (fold-change >2.0) for each NUP98-translocated cohort (*Online Supplementary Table S7*). This revealed a transcriptional network in *NUP98-KDM5A* with *GATA1* and *GATA2* both highly upregulated compared to the reference cohort, and their downstream target genes concomitantly overexpressed, with concurrent downregulation of *ERG*, which is known to have an inverse relationship with *GATA* expression.[39]

DNA methylation profiling

We analyzed DNA methylation data from 334,934 CpG probes. We then performed dimensionality reduction using non-negative matrix factorization (NMF) and used UMAP to determine how the variation in DNA methylation associates with *NUP98* fusion groups and normal bone marrow (NBM). We found that *NUP98* fusion groups cluster together (Figure 5A). Specifically, the HOX-activating fusions (*NSD1, HOX*, and *PRRX1*) form a unique cluster, and also the fusion partners with reader-like functions (*BPTF, BRWD3, DDX10, HMGB3, KAT7, PHF15, PHF23, SET*, and *TOP1*) cluster together. The reader-like fusions also cluster more closely to NBM. By performing unsupervised clustering of the NMF factors that associate with each group, we found that the *NUP98-HOX*-like group clusters distinctly from the *NUP98*-readers and NBM, further illustrating that *NUP98* fusions differ in methylation profiles (Figure 5B).

We further analyzed the NMF factors that associate significantly with the *NUP98-HOX*, *NUP98*-Reader, and *NUP98*-Reader plus abn13 groups (Figure 5C). In order to identify the defining characteristics within each of these factors, we performed enrichment analyses against chromatin states, histone marks, and transcription factor binding sites (Figure 5D). The *NUP98-HOX* group enrichments in NMF 3 indicate that these fusions lead to Polycomb-mediated hypermethylation at actively transcribed genes, evidenced by H2AK119ub, H3K23me2, H3K36me2/3, and H3K27me3 enrichment at binding motifs for *RYBP* (a subunit of Polycomb repressor complex 1). This likely occurs because H3K36me2/3 increases throughout the *HOXA/B* clusters and at *HOX* targets, while H3K27me3 peaks disappear as hyperactive *NSD1* displaces PRC1/2 from the *HOX* clusters. This may result in reducing expressing potential and arresting cellular differentiation, which often coincides with loss of imprinting, as evidenced by dual enrichment for H3K27me3 and H3K36me3, as well as transcription factor binding site enrichment for *ZFP57*, the master regulator of genomic imprinting control regions.

The enrichment of NMF 6 suggests that *NUP98*-Reader fusions likely lead to localization of transcriptional condensates at already highly expressed developmental genes, leading to an enrichment of DNA hypermethylation in transcribed exons.

The enrichment of NMF 8 suggests that abnormal chr13 cases, all of which are NUP98-Reader fusions, show additional hypermethylation of actively expressed gene bodies, evidenced by enrichment for H3K36me3 and H2BK120ub, along with loss of imprinting (though far less pronounced than in *NUP98-HOX* fusions), which is evidenced by an enrichment for *ZFP57* binding sites.

Clinical outcome and prognostic relevance

We evaluated the impact of *NUP98* translocations on response to initial induction therapy. Overall, the morphologic CR rate after course one for the *NUP98* fusion cohort was 50% *versus* 78% for the reference cohort ($P<0.001$). *NUP98-NSD1* patients had a significantly lower CR rate of 38% ($P<0.001$) compared the reference cohort, while *NUP98-*

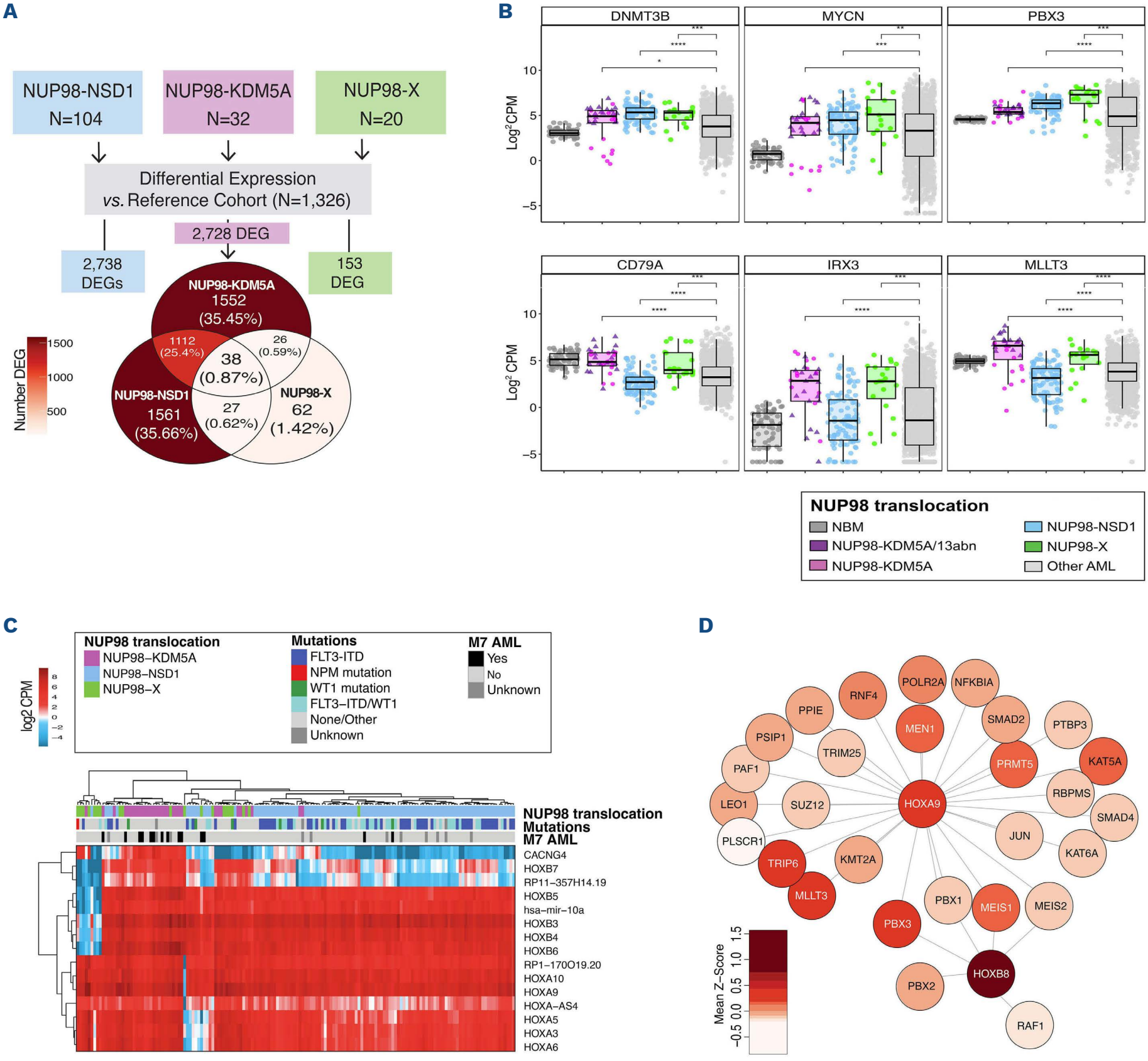

Figure 4. Differential expression of all *NUP98*-translocated pediatric acute myeloid leukemia patients. (A) Schematic of differential expression analyses completed for *NUP98*-translocated samples. The overlap of differentially expressed genes (DEG) identified in each *NUP98* cohort is represented in the Venn diagram. (B) DEG between *NUP98*-translocated AML groups compared to the reference cohort and normal bone marrow (NBM) were identified. Subsets of dysregulated genes were commonly identified in both *NUP98*-X and *NUP98*-NSD1 (upper panel) or were identified as shared between *NUP98*-X and *NUP98-KDM5A* (lower panel). (C) Commonly DEG found in all three *NUP98*-translocated pediatric acute myeloid leukemia (AML) subgroups. (D) Mean expression (Z-score transformed) of *HOXA9* and *HOXB8* interacting partners in *NUP98*-X translocated AML. The darker shades of red indicate higher expression in the *NUP98*-X cohort. CPM: counts per million.

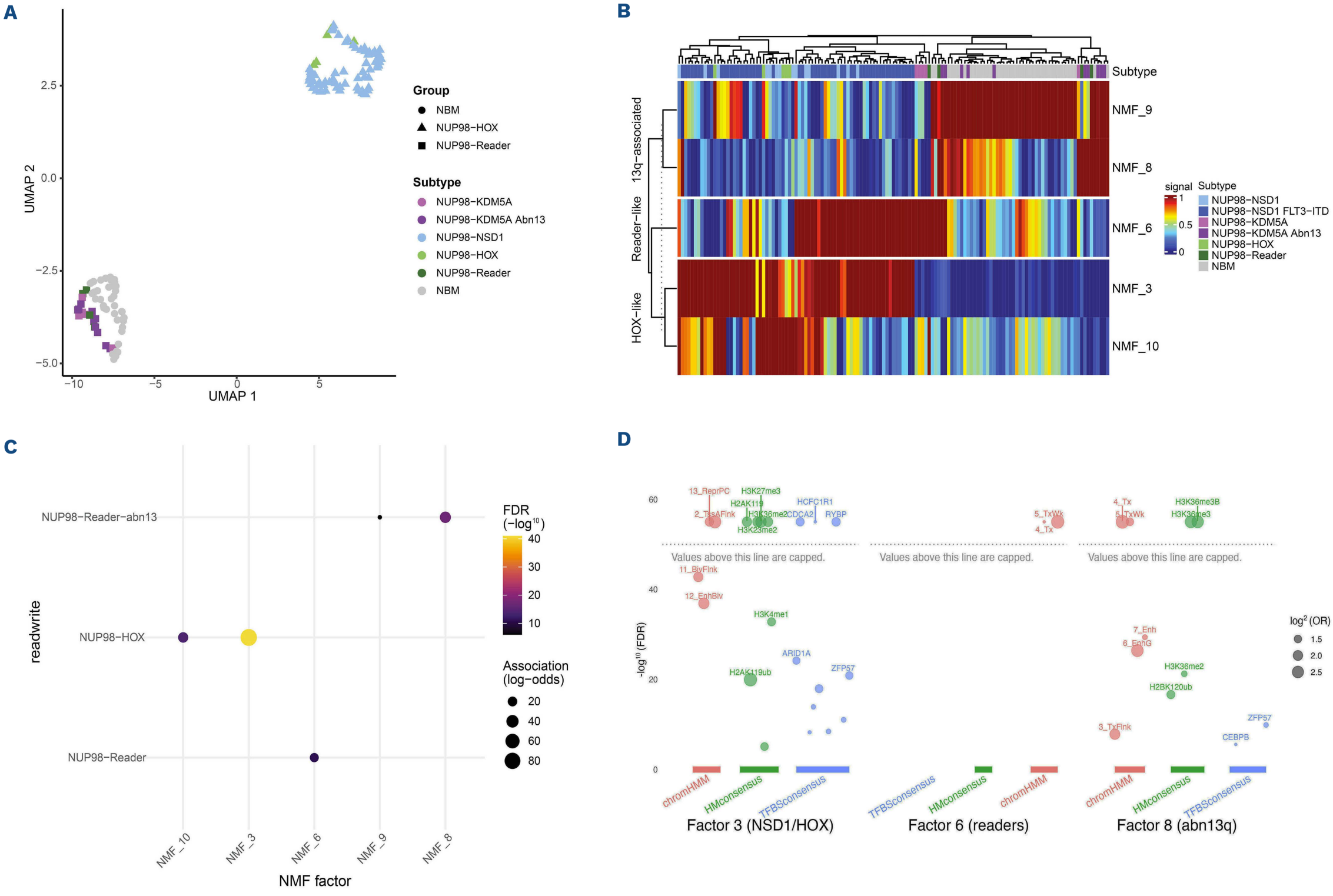

Figure 5. DNA methylation of pediatric acute myeloid leukemia patients with *NUP98* translocations. (A) Uniform manifold approximation and projection (UMAP) of DNA methylation data in *NUP98*-translocated acute myeloid leukemia (AML) subgroups compared to the reference cohort and normal bone marrow (NBM). (B) Heatmap of non-negative matrix factorizations (NMF) of DNA methylation data. The NMF factors are those that were significantly associated with *NUP98* translocation AML subgroups. (C) NMF factor associations of DNA methylation with *NUP98-HOX*-like fusions (*NUP98-NSD1*, *NUP98-HOX*, and *NUP98-PRRX1*) and *NUP98*-Reader-like fusions (*NUP98-KDM5A*, *NUP98- BPTF, NUP98-BRWD3, NUP98-DDX10, NUP98-KAT7, NUP98- PHF15, NUP98-SET,* and *NUP98-TOP1*) with or without a co-occuring abnormal chromosome 3 (chr3). (D) NMF factor enrichments of DNA methylation for chromatin states, chromatin marks, and transcription factor binding sites. Factor 3 is enriched in *NUP98-HOX*-like fusions, factor 6 is enriched in *NUP98*-Reader-like fusions, and factor 8 is enriched in *NUP98*-Reader-like fusions with an abnormal chr13. FDR: false discovery rate; OR: odds ratio; ReprPC: repressed PolyComb; TssAFlank: flanking active TSS, BivFlank: flanking bivalent; TSS/Enh, EnhBiv: bivalent enhancer; TxWk: weak transcription; Tx: Strong transcription; Enh: enhancers; EnhG: genic enhancers.

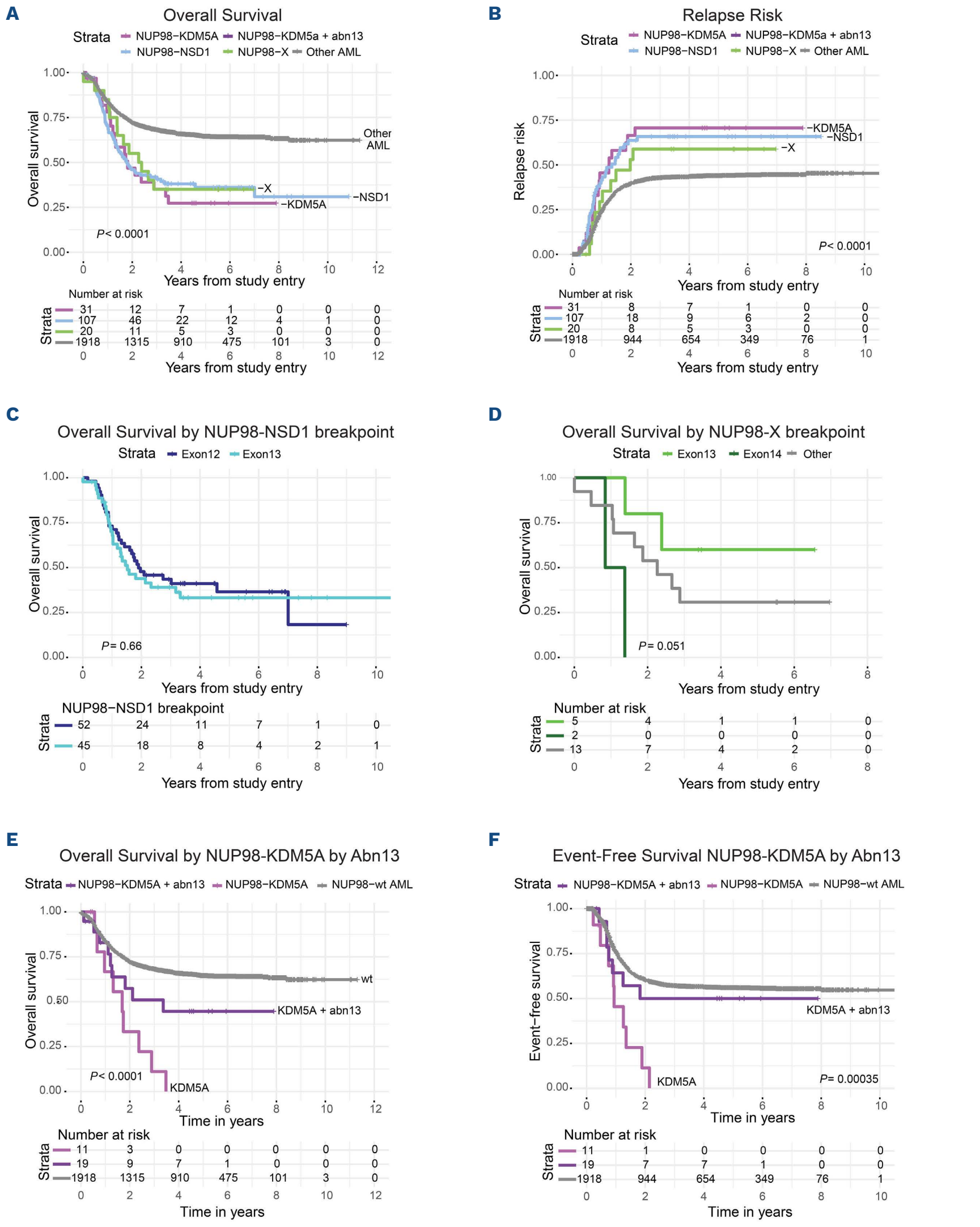

Figure 6. Survival of pediatric acute myeloid leukemia patients with NUP98 translocations. Kaplan Meier estimates of (A) overall survival (OS) and (B) relapse risk (RR) of pediatric *NUP98*-translocated acute myeloid leukemia (AML) patients with different translocation partners compared to a reference cohort without *NUP98* fusions. OS of (C) *NUP98-NSD1* and (D) *NUP98*-X, when divided by *NUP98* fusion exon breakpoint. Outcome was also examined for (E) OS and (F) event-free survival (EFS) of *NUP98-KDM5A* subgroups by chromosome 13 (chr13) status (monosomy 13, del(13q), translocation 13). Abn3: abnormal chr 3.

KDM5A and *NUP98*-X had CR rates of 81% (*P*=0.729) and 65% (*P*=0.176), respectively. *NUP98-NSD1* and *NUP98-KDM5A* patients had significantly higher evidence of MRD (73%; *P*<0.001, and 52%; *P*=0.005, respectively), while this was similar to the reference cohort in *NUP98*-X (22% *vs*. 27%; *P*=0.793).

The 5-year OS for the *NUP98* fusion cohort was 35% *versus* 64% for the reference group (*P*<0.001). *NUP98-NSD1* patients had inferior OS (36% *vs*. 64%, *P*<0.001) and event-free survival (EFS) (17% *vs*. 47%; *P*<0.001) compared to the reference (*Online Supplementary Table S1;* Figure 6A, B). Similarly, adverse outcomes for *NUP98-KDM5A* were observed for OS (30%; *P*<0.001) and EFS (25%; P=0.01). *NUP98-NSD1* and *NUP98-KDM5A* cases showed a significantly higher 5-year relapse risk (RR) of 64% (*P*=0.001) and 68% (*P*=0.010) respectively, compared to the reference cohort (42%) (Figure 6B). *NUP98*-X displayed a similar inferior OS (35%; *P*=0.009); however, EFS (35%; *P*=0.333) and RR (69%; *P*=0.071) differences did not reach significant difference. Response to treatment in *NUP98*-translocated subgroups, examined by disease-free survival (DFS) estimates 5 years after induction one, was lower compared to the reference cohort (27% vs. 52%; *P*<0.001). This held true for all subsets; *NUP98-NSD1* (28%; *P*<0.001), *NUP98-KDM5A* (28%; *P*=0.012) and *NUP98*-X (23%; *P*=0.044) (*Online Supplementary Figure S9A*).

Multivariable cox regression analyses were performed to adjust for cytomolecular risk groups, white blood cells, and different *NUP98*-translocated subgroups (*Online Supplementary Table S8*). After correction, significantly inferior OS (hazard ratio [HR]=1.463; 95% confidence interval [CI]: 1.1-1.94; *P*=0.009), EFS (HR=2.032; 95% CI: 1.59-2.59; *P*<0.001) and RR (HR=1.743; 95% CI: 1.1-2.76; *P*=0.018) were observed in *NUP98-NSD1* patients compared to the reference group. Also, *NUP98-KDM5A* (HR=1.825; 95% CI: 1.13-2.96; *P*=0.015) and *NUP98*-X patients (HR=1.75; 95% CI: 1.01-3.04; *P*=0.046) showed poor OS, without significant differences in EFS and RR.

We examined outcomes corresponding to fusion exon junctions (Figure 6C, D; *Online Supplementary Figure 9A, B*). There were no significant differences in outcome for *NUP98-NSD1* or *NUP98*-X by exon junction, though a trend toward improved outcomes was observed for *NUP98*-X exon 13 breakpoints. *NUP98-KDM5A* patients with exon 13 junctions (n=19) had an OS of 51% compared to 0% for exon 14 breakpoints (n=12; *P*=0.011) with corresponding EFS (40% *vs*. 0%, respectively; *P*=0.174). Due to high concurrence of chr13 alterations with exon 13 junctions, a similar trend was observed in *NUP98-KDM5A*/13abn compared to *NUP98-KDM5A*/13normal patients (EFS 45% *vs*. 0%; *P*=0.052). *NUP98-KDM5A* patients had a worse prognosis compared to the reference cohort without *NUP98* fusions regardless of chr13 alterations; however, the presence of chr13 alterations within the *NUP98-KDM5A* group was associated with increased OS and EFS (Figure 6E, F).

Discussion

NUP98-translocated pAML has emerged as a distinct but heterogeneous group, and a comprehensive study defining varied fusion partners, phenotypes, transcript subclasses and outcomes was still lacking. Incorporation of genome, transcriptome, methylation, and clinical data from several large pediatric and adult AML studies provided deep insight into this family of fusions. Our study demonstrates that the underlying biology of *NUP98*-translocated AML is defined by the fusion partner. Furthermore, although fusions involving *NSD1* and *KDM5A* are cryptic, an overwhelming majority of *NUP98*-X fusions can be identified by conventional karyotype, facilitating identification at diagnosis.

Importantly, we identified a significant overlap of cooperating lesions including mutations (*FLT3, WT1*) and karyotypic alterations (trisomy 8, del13q). We confirmed prior observation of substantial enrichment of *FLT3*-ITD in *NUP98-NSD1* patients (80%). This extreme prevalence, and *NUP98-NSD1* preceding *FLT3*-ITD, suggest a causal relationship; this intriguing hypothesis is being studied in our laboratory.

Recently, exon usage and fusion junctions were shown to have clinical and biological implications; patients with a *CBFB-MYH11* fusion with the common exon 5/33 breakpoint had significantly inferior EFS than those with less common fusion junctions.[40] We here demonstrated that patients with *NUP98-KDM5A* with exon 13 involvement had a more favorable prognosis. However, the strong association of exon 13 usage with chr13 alterations in *NUP98-KDM5A* patients makes it difficult to discern which of these factors is underlying this outcome difference (Figure 6; *Online Supplementary Figure S9*). The difference that we discovered in prognosis may suggest that *NUP98-KDM5A* cases with or without exon 13 breakpoints and chr13 abnormalities could be divided into different subgroups. The observation that *NUP98-KDM5A*/abn13 patients have a more favorable prognosis potentially affects treatment stratification of these patients in future. Furthermore, these findings provide a rationale that future studies must go beyond simple defining the presence or absence of a fusion and investigate specific exon usage, inclusion/exclusion of critical functional domains, and functionality of the oncoprotein.

Transcriptome profiling further defined functional classifications of *NUP98* fusions. Expression of *PRDM16* and *MECOM* could clearly segregate *NUP98*-translocated subsets. *PRDM16* and *MECOM* encode H3K9-mono□methyltransferases that are important in the maintenance of heterochromatin integrity and are selectively expressed in hematopoietic stem cells (HSC)[36] and linked to oncogenic transformation;[41] their deregulation could play a role in leukemogenesis of *NUP98* translocations. Gene expression profiling also revealed distinct expression networks defined by translocation partner and cooperating mutations/alterations. Not only did *NUP98-KDM5A* patients cluster based on abn13, bimodal expression

of *DNMT3B, MYCN, MECOM*, and *PRDM16* was associated with abn13. Interestingly, where *PRDM16* is a poor prognostic factor in AML,[36] high expression was associated with *NUP98-KDM5A*/abn13, which had a better prognosis in our cohort. This association may indicate different molecular pathways underlying leukemogenesis within *NUP98-KDM5A*, where *NUP98-KDM5A*/13abn may have more immature HSC-like features.

Regardless of fusion partner, *NUP98* translocations shared overexpression of *HOXA/B* genes. The translocation partners *KDM5A* and *PHF23* contain PHD protein domains, which function in histone methylation and nucleosome remodelling.[25] The HOX cluster was shown to be in a locked, transcriptionally active position due to the H3K4me3-binding PHD-domain when fused to *NUP98*[25] and this may be extendable to the leukemogenic ability of *PHF15* and *BPTF*, which retain their PHD finger. Translationally, upregulation of the *HOXA* cluster indicates a potential therapeutic role of menin-inhibitors in *NUP98*-translocated AML, as has been recently shown in mice[42] and *in vitro* studies of primary pAML samples.[43]

Chromatin modifiers, such as *NSD1* and *KDM5A*, are frequently the targets of oncogenic fusions in pediatric disease.[44] DNA methylation profiling suggests that rare and diverse *NUP98*-X fusions share one of the two key mechanisms to promote leukemogenesis: either by activating the *HOX* genes and their targets and promoting loss of genomic imprinting (like *NUP98-NSD1*), or by directing transcriptional machinery to developmentally inappropriate targets (as seen in *NUP98-KDM5A* fusions and chromatin reader fusions). The mutational, structural, transcriptional, and epigenomic signatures of these two major groups of *NUP98* fusion partners are so starkly distinct that one cannot help but speculate that each group should be treated as a separate subtype of AML, where both common and rare partners are likely to respond to similar treatments, whether repurposed (disulfiram for chromatin reader fusions) or novel (*CDK9* inhibitors for *HOX* fusions).

Overall, *NUP98* fusions constitute a highly refractory class of AML, which justifies reclassification of *NUP98* fusions, regardless of fusion partner, as a high-risk subtype in future trials. Further research may focus on *NUP98* fusion cases with aberrations of chr13, typically co-occurring with *NUP98* exon 13 breakpoints and a distinctive immunophenotype, whose outcomes are relatively favorable given standard of care induction and/or transplantation. The balance of *NUP98* fusions, with or without characteristic co-occurring mutations, remains an urgent, unmet therapeutic need. The immunophenotype, transcriptome, and epigenome of HOX-activating (*versus* chromatin-reader) fusion partners may provide important leads towards more effective therapies, while their signatures may permit rapid discontinuation of ineffective therapies in this high-risk group of patients.

Disclosures

AJM, LEB and LP are employees/paid consultants for Hematologics Inc.. MRL is an employee/paid consultant for and holds ownership interest in Hematologics. All other authors have no conflicts of interest to disclose.

Contributions

BFG and SM supervised the study. HH, MD, CW, NM and CM included additional patient data. JLS, LH, YJW, AJM, TJT, XM, TIS, RER, ARL, and ELP processed and analyzed the data. EJMB and JLS drafted the manuscript. All authors edited and approved the manuscript.

Acknowledgments

The authors wish to gratefully acknowledge the important contributions of the late Dr. Stephen H. Petersdorf to SWOG and to the study S0106.

Funding

This work was supported by the following NIH/NCI/NCTN grant awards: RO1CA190661, R01CA160872, R01AI171984, U10CA180888, U10CA180819, and U24CA196175, U10CA180886, U10CA180899, St. Baldricks Foundation, the Rally Foundation, and the Michelle Lunn Hope Foundation. This content is solely the responsibility of the authors and does not necessarily represent the official views of the National Institutes of Health.

Data-sharing statement

RNA-sequencing and DNA methylation array data on primary patient samples, as well as associated clinical/outcome data, are deposited in Genomic Data Commons (GDC, https://portal.gdc.cancer.gov/) and the Target Data Matrix (https://ocg.cancer.gov/programs/target/data-matrix) under project ID "TARGET-AML". Access to protected files hosted on the Sequence Read Archive (SRA), such as raw sequencing data in bam or fastq format, are available through dbGaP TARGET: Acute Myeloid Leukemia study (accession: phs000465.v20.p8). Additional DNA methylation data are hosted on the Gene Expression Omnibus (GEO) under accessions GSE190931 and GSE124413. The Beat AML Study controlled access RNA-sequencing data were downloaded from the Genomic Data Commons (GDC) portal and are available through the Functional Genomic Landscape of Acute Myeloid Leukemia study on dbGaP (accession: phs001657.v1.p1). TCGA LAML RNA-sequencing fusion data were accessed from the GDC Data Portal (https://gdc.cancer.gov/about-data/publications/laml_2012).

References

1. Balgobind BV, Hollink IH, Arentsen-Peters ST, et al. Integrative analysis of type-I and type-II aberrations underscores the genetic heterogeneity of pediatric acute myeloid leukemia. Haematologica. 2011;96(10):1478-1487.
2. Zwaan CM, Kolb EA, Reinhardt D, et al. Collaborative efforts driving progress in pediatric acute myeloid leukemia. J Clin Oncol. 2015;33(27):2949-2962.
3. de Rooij JD, Zwaan CM, van den Heuvel-Eibrink M. Pediatric AML: from biology to clinical management. J Clin Med. 2015;4(1):127-149.
4. Creutzig U, Zimmermann M, Ritter J, et al. Treatment strategies and long-term results in paediatric patients treated in four consecutive AML-BFM trials. Leukemia. 2005;19(12):2030-2042.
5. Michmerhuizen NL, Klco JM, Mullighan CG. Mechanistic insights and potential therapeutic targets for NUP98-rearranged hematologic malignancies. Blood. 2020;136(20):2275-2289.
6. Nakamura T, Largaespada DA, Lee MP, et al. Fusion of the nucleoporin gene NUP98 to HOXA9 by the chromosome translocation t(7;11)(p15;p15) in human myeloid leukaemia. Nat Genet. 1996;12(2):154-158.
7. Gough SM, Slape CI, Aplan PD. NUP98 gene fusions and hematopoietic malignancies: common themes and new biologic insights. Blood. 2011;118(24):6247-6257.
8. Struski S, Lagarde S, Bories P, et al. NUP98 is rearranged in 3.8% of pediatric AML forming a clinical and molecular homogenous group with a poor prognosis. Leukemia. 2017;31(3):565-572.
9. Hollink IH, van den Heuvel-Eibrink MM, Arentsen-Peters ST, et al. NUP98/NSD1 characterizes a novel poor prognostic group in acute myeloid leukemia with a distinct HOX gene expression pattern. Blood. 2011;118(13):3645-3656.
10. de Rooij JD, Branstetter C, Ma J, et al. Pediatric non-Down syndrome acute megakaryoblastic leukemia is characterized by distinct genomic subsets with varying outcomes. Nat Genet. 2017;49(3):451-456.
11. Jaju RJ, Fidler C, Haas OA, et al. A novel gene, NSD1, is fused to NUP98 in the t(5;11)(q35;p15.5) in de novo childhood acute myeloid leukemia. Blood. 2001;98(4):1264-1267.
12. de Rooij JD, Hollink IH, Arentsen-Peters ST, et al. NUP98/JARID1A is a novel recurrent abnormality in pediatric acute megakaryoblastic leukemia with a distinct HOX gene expression pattern. Leukemia. 2013;27(12):2280-2288.
13. Noort S, Wander P, Alonzo TA, et al. The clinical and biological characteristics of NUP98-KDM5A in pediatric acute myeloid leukemia. Haematologica. 2020;106(2):630-634.
14. Lange BJ, Smith FO, Feusner J, et al. Outcomes in CCG-2961, a children's oncology group phase 3 trial for untreated pediatric acute myeloid leukemia: a report from the children's oncology group. Blood. 2008;111(3):1044-1053.
15. Cooper TM, Franklin J, Gerbing RB, et al. AAML03P1, a pilot study of the safety of gemtuzumab ozogamicin in combination with chemotherapy for newly diagnosed childhood acute myeloid leukemia: a report from the Children's Oncology Group. Cancer. 2012;118(3):761-769.
16. Aplenc R, Meshinchi S, Sung L, et al. Bortezomib with standard chemotherapy for children with acute myeloid leukemia does not improve treatment outcomes: a report from the Children's Oncology Group. Haematologica. 2020;105(7):1879-1886.
17. Pollard JA, Loken M, Gerbing RB, et al. CD33 expression and its association with gemtuzumab ozogamicin response: results from the randomized phase III Children's Oncology Group Trial AAML0531. J Clin Oncol. 2016;34(7):747-755.
18. Tyner JW, Tognon CE, Bottomly D, et al. Functional genomic landscape of acute myeloid leukaemia. Nature. 2018;562(7728):526-531.
19. Ley TJ, Miller C, Ding L, et al. Genomic and epigenomic landscapes of adult de novo acute myeloid leukemia. N Engl J Med. 2013;368(22):2059-2074.
20. Anderson JE, Kopecky KJ, Willman CL, et al. Outcome after induction chemotherapy for older patients with acute myeloid leukemia is not improved with mitoxantrone and etoposide compared to cytarabine and daunorubicin: a Southwest Oncology Group study. Blood. 2002;100(12):3869-3876.
21. Petersdorf SH, Rankin C, Head DR, et al. Phase II evaluation of an intensified induction therapy with standard daunomycin and cytarabine followed by high dose cytarabine for adults with previously untreated acute myeloid leukemia: a Southwest Oncology Group study (SWOG-9500). Am J Hematol. 2007;82(12):1056-1062.
22. Godwin JE, Kopecky KJ, Head DR, et al. A double-blind placebo-controlled trial of granulocyte colony-stimulating factor in elderly patients with previously untreated acute myeloid leukemia: a Southwest Oncology Group study (9031). Blood. 1998;91(10):3607-3615.
23. List AF, Kopecky KJ, Willman CL, et al. Benefit of cyclosporine modulation of drug resistance in patients with poor-risk acute myeloid leukemia: a Southwest Oncology Group study. Blood. 2001;98(12):3212-3220.
24. Haas BJ, Dobin A, Li B, et al. Accuracy assessment of fusion transcript detection via read-mapping and de novo fusion transcript assembly-based methods. Genome Biol. 2019;20(1):213.
25. Robertson G, Schein J, Chiu R, et al. De novo assembly and analysis of RNA-seq data. Nat Methods. 2010;7(11):909-912.
26. Tian L, Li Y, Edmonson MN, et al. CICERO: a versatile method for detecting complex and diverse driver fusions using cancer RNA sequencing data. Genome Biol. 2020;21(1):126.
27. Robinson JT, Thorvaldsdóttir H, Winckler W, et al. Integrative genomics viewer. Nat Biotechnol. 2011;29(1):24-26.
28. Thorvaldsdóttir H, Robinson JT, Mesirov JP. Integrative Genomics Viewer (IGV): high-performance genomics data visualization and exploration. Brief Bioinform. 2013;14(2):178-192.
29. Robinson JT, Thorvaldsdóttir H, Wenger AM, Zehir A, Mesirov JP. Variant review with the integrative genomics viewer. Cancer Res. 2017;77(21):e31-e34.
30. Robinson JT, Thorvaldsdóttir H, Turner D, Mesirov JP. igv.js: an embeddable JavaScript implementation of the Integrative Genomics Viewer (IGV). Bioinformatics. 2023;39(1):btac830.
31. Edmonson MN, Zhang J, Yan C, et al. Bambino: a variant detector and alignment viewer for next-generation sequencing data in the SAM/BAM format. Bioinformatics. 2011;27(6):865-866.
32. Chisholm KM, Heerema-McKenney AE, Choi JK, et al. Acute erythroid leukemia is enriched in NUP98 fusions: a report from the Children's Oncology Group. Blood Adv. 2020;4(23):6000-6008.
33. Eidenschink Brodersen L, Alonzo TA, Menssen AJ, et al. A recurrent immunophenotype at diagnosis independently identifies high-risk pediatric acute myeloid leukemia: a report from Children's Oncology Group. Leukemia. 2016;30(10):2077-2080.
34. Ostronoff F, Othus M, Gerbing RB, et al. NUP98/NSD1 and FLT3/ITD coexpression is more prevalent in younger AML patients and leads to induction failure: a COG and SWOG report. Blood. 2014;124(15):2400-2407.
35. Traag VA, Waltman L, van Eck NJ. From Louvain to Leiden: guaranteeing well-connected communities. Sci Rep. 2019;9(1):5233.

36. Shiba N, Ohki K, Kobayashi T, et al. High PRDM16 expression identifies a prognostic subgroup of pediatric acute myeloid leukaemia correlated to FLT3-ITD, KMT2A-PTD, and NUP98-NSD1: the results of the Japanese Paediatric Leukaemia/Lymphoma Study Group AML-05 trial. Br J Haematol. 2016;172(4):581-591.
37. Barbie DA, Tamayo P, Boehm JS, et al. Systematic RNA interference reveals that oncogenic KRAS-driven cancers require TBK1. Nature. 2009;462(7269):108-112.
38. Dard A, Reboulet J, Jia Y, et al. Human HOX proteins use diverse and context-dependent motifs to interact with TALE class cofactors. Cell Rep. 2018;22(11):3058-3071.
39. Thirant C, Ignacimouttou C, Lopez CK, et al. ETO2-GLIS2 hijacks transcriptional complexes to drive cellular identity and self-renewal in pediatric acute megakaryoblastic leukemia. Cancer Cell. 2017;31(3):452-465.
40. Huang BJ, Smith JL, Wang YC, et al. CBFB-MYH11 fusion transcripts distinguish acute myeloid leukemias with distinct molecular landscapes and outcomes. Blood Adv. 2021;5(23):4963-4968.
41. Ivanochko D, Halabelian L, Henderson E, et al. Direct interaction between the PRDM3 and PRDM16 tumor suppressors and the NuRD chromatin remodeling complex. Nucleic Acids Res. 2019;47(3):1225-1238.
42. Heikamp EB, Henrich JA, Perner F, et al. The Menin-MLL1 interaction is a molecular dependency in NUP98-rearranged AML. Blood. 2022;139(6):294-906.
43. Rasouli M, Szoltysek K, Cameron R, et al. NUP98/NSD1-positive AML is addicted to functional Menin-MLL interaction. EHA Library. 06/09/21;325136;EP382.
44. Bolouri H, Farrar JE, Triche T, Jr., et al. The molecular landscape of pediatric acute myeloid leukemia reveals recurrent structural alterations and age-specific mutational interactions. Nat Med. 2018;24(1):103-112.